



## New small-size peptides possessing antifungal activity

Francisco M. Garibotto<sup>a,b</sup>, Adriana D. Garro<sup>a,b</sup>, Marcelo F. Masman<sup>a,c</sup>, Ana M. Rodríguez<sup>a</sup>, Paul G. M. Luiten<sup>c</sup>, Marcela Raimondi<sup>d</sup>, Susana A. Zacchino<sup>d</sup>, Csaba Somlai<sup>e</sup>, Botond Penke<sup>e</sup>, Ricardo D. Enriz<sup>a,b,\*</sup>

<sup>a</sup> Facultad de Química, Bioquímica y Farmacia, Universidad Nacional de San Luis, Chacabuco 915, 5700 San Luis, Argentina

<sup>b</sup> IMBIO-SL, CONICET, Chacabuco 915, 5700 San Luis, Argentina

<sup>c</sup> Department of Molecular Neurobiology, University of Groningen, Kerklaan 30, 9751 NN Haren, The Netherlands

<sup>d</sup> Facultad de Ciencias Bioquímicas y Farmacéuticas, Farmacognosia, Universidad Nacional de Rosario, Suipacha 531, Rosario 2000, Argentina

<sup>e</sup> Department of Medical Chemistry, University of Szeged H-6720 Szeged, Dom Tér 8, H-6720 Szeged, Hungary

### ARTICLE INFO

#### Article history:

Received 3 September 2009

Revised 3 November 2009

Accepted 4 November 2009

Available online 10 November 2009

#### Keywords:

Small-size peptides

Antifungal activity

Conformational study

Molecular electrostatic potentials

### ABSTRACT

The synthesis, in vitro evaluation, and conformational study of a new series of small-size peptides acting as antifungal agents are reported. In a first step of our study we performed a conformational analysis using Molecular Mechanics calculations. The electronic study was carried out using Molecular electrostatic potentials (MEPs) obtained from RHF/6-31G calculations. On the basis of the theoretical predictions three small-size peptides, RQWKKWWQWRR-NH<sub>2</sub>, RQJRRWWQWRR-NH<sub>2</sub>, and RQJRRWWQW-NH<sub>2</sub> were synthesized and tested. These peptides displayed a significant antifungal activity against human pathogenic strains including *Candida albicans* and *Cryptococcus neoformans*. Our experimental and theoretical results allow the identification of a topographical template which can serve as a guide for the design of new compounds with antifungal properties for potential therapeutic applications against these pathogenic fungi.

© 2009 Elsevier Ltd. All rights reserved.

### 1. Introduction

Fungal infections pose a continuous and serious threat to human health and life especially to immunocompromised patients.<sup>1–3</sup> Many fungal infections are caused by opportunistic pathogens that may be endogenous (*Candida* infections) or acquired from the environment (*Cryptococcus*, *Aspergillus* infections). Patients with significant immunosuppression frequently develop *Candida* esophagitis, while cryptococcosis, caused by the encapsulated yeast *Cryptococcus neoformans*, has been the leading cause of fungal mortality among patients with reduced immune defence mechanisms. The latter fungal species has predilection for the central nervous system and its infection leads to severe, life-threatening meningitis. McNeil et al.<sup>4</sup> found a dramatic increase in mortality between 1980 and 1997 due to mycoses from multiple origins, which could mainly be associated with *Candida*, *Aspergillus*, and *Cryptococcus* genera. However, besides these known fungal species, new emerging fungal pathogens appear every year as the cause of morbidity and life-threatening infections in the immunocompromised hosts.<sup>1,5</sup>

Although different antifungal agents are available for the treatment of fungal infections, some of them have undesirable side ef-

fects, are ineffective against new or re-emerging fungi or develop resistance mainly due to the broad use of antifungal drugs.<sup>6</sup> Although combination therapy has emerged as a good alternative to bypass these disadvantages,<sup>7,8</sup> there is an urgent need for a next generation of safer and more potent antifungal agents.<sup>1,8</sup> This need has resulted in the identification of novel molecules, with a promise for future therapeutic development. Both natural and synthetic peptides have gained attention as potential new antifungal agents.<sup>9,10</sup> These peptides proved to be able to inhibit a broad spectrum of pathogens and microorganisms<sup>11–13</sup> and, importantly, without inducing bacterial or fungal resistance.<sup>14</sup> Among them, some natural peptides were recently identified as antifungal compounds that showed to inhibit a broad spectrum of pathogenic microorganisms.<sup>15–18</sup> It has been reported that a group of cationic antimicrobial peptides are major players in the innate immune response.<sup>19,20</sup> These peptides appear to represent very ancient elements of the immune response of all living species and the induction pathways for these compounds in vertebrates, insects, and plants<sup>19–21</sup> are highly conserved. Furthermore, it is becoming increasingly clear that cationic antimicrobial peptides have many potential roles in inflammatory responses, which represent an orchestration of the mechanisms of innate immunity.

Small cationic peptides<sup>12,22</sup> are abundant in nature and have been described as 'nature's antibiotics' or 'cationic antimicrobial peptides'. These peptides are 12–50 amino acids long with a net

\* Corresponding author.

E-mail address: [denriz@unsl.edu.ar](mailto:denriz@unsl.edu.ar) (R.D. Enriz).

positive charge of +2 or +9, which is due to an excess of basic arginine and lysine residues, and approximately 50% hydrophobic amino acids.<sup>12</sup> These molecules are folded in three dimensions so that they have both a hydrophobic face comprising non-polar amino acid side-chains, and a hydrophilic face of polar and positively charged residues: these molecules are amphipathic. Despite these two similarities these compounds vary considerably in length, amino acid sequence, and secondary structure. The different spatial orderings include small  $\beta$ -sheets stabilized by disulfide bridges, amphipathic  $\alpha$ -helices and, less commonly, extended and loop structures.

Recently we reported that penetratin, a well-known cell penetrating peptide, displayed a significant antifungal effect against both *Candida albicans* and *C. neoformans* two important life-threatening infections for immunocompromised hosts.<sup>23</sup> The consideration that a peptide-based antifungal agent should be as short as possible in order to reduce its production costs, prompted us to synthesize shorter derivatives of penetratin. Within that framework we synthesized shorter peptides structurally related with penetratin but those small-size peptides showed to be inactive or yielded only a marginal antifungal effects. In fact, only the tetrapeptide RQKK displayed a moderate antifungal activity against *C. neoformans* and was practically inactive against *C. albicans*.<sup>23</sup> On the basis of these previous results, in the present study we aimed at developing a next generation of small-size peptides possessing antifungal properties that may be, at least, comparable to those of penetratin against *C. albicans* and *C. neoformans*. To characterize the structure–antifungal activity relationship of these compounds, in the present investigation we explored the influence of amino acid substitutions and deletions on its antifungal activity. In addition, a conformational and electronic analysis of this new series of peptides was carried out using theoretical calculations. This study was performed in order to identify a topographical and/or substructural template, which can be the starting structure for the design of new antifungal peptides.

## 2. Results and discussion

As stated above the principal aim of this study is to develop new antifungal peptides possessing a length as short as possible while maintaining their antifungal activity. Thus, on the basis of our previous results,<sup>23</sup> the RQKK sequence was selected as the starting structure, since RQKK was the smallest peptide so far showing at least a moderate antifungal effect against *C. neoformans*. Therefore, we performed sequential changes on RQKK in order to obtain information on the potential role of each amino acid in the sequence.

Figure 1 shows in a schematic way how the different amino acids of RQKK were replaced in a kind of ‘point mutation’ procedure. These structural changes were designed without any consideration about the possible changes in the physicochemical properties introduced with each structural modification. None of these 12 tetrapeptides obtained by this way (compounds **1–12**), except the previously reported RQKK (**10**), displayed any significant antifungal effect against *C. neoformans*. They do not completely inhibit the growth of *C. neoformans* even at high concentrations, showing percentages of inhibition ranging from 3.72% to 78.6% at the highest concentration tested for compounds **1–9** and **11–12** thus possessing a Minimum Inhibitory Concentration (MIC) above 200  $\mu$ M (Table 1). This low activity prompted us to develop new small-size peptides using a rational design based on theoretical calculations.

In our previous paper we performed a detailed conformational and electronic study for penetratin and its derivatives.<sup>23</sup> These results allowed us to identify a possible ‘biologically relevant conformation’ or ‘pharmacophoric patron’ for these peptides. A particular combination of cationic and hydrophobic residues adopting a definite spatial ordering appeared to be the key parameter for the membrane transition from hydrophilic to hydrophobic phase, which could be an essential and necessary step to produce the antifungal activity. Considering these previous results we decided to synthesize a peptide, smaller than penetratin but larger than RQKK, able to adopt the pharmacophoric patron displayed by penetratin.

In our initial studies we maintained the same number of cationic amino acids (R and K) as in penetratin (compound **13**), deleting Q2, I3, I5, F7, Q8, N9, and M12. This way we obtained and tested compounds **14–17** which displayed a markedly lower antifungal activity compared to compound **13** (Table 2). In fact, only peptides **14** and **16** showed a marginal effects against *C. neoformans* and *C. albicans* inhibiting 68%, 76%, and 33% at 100  $\mu$ M and MICs (100% inhibition) = 200  $\mu$ M, while the others may be considered as inactive compounds. Observing the MEPs previously reported for compounds **14–17** it is clear that these peptides appears to be ‘too cationic’ displaying a dominant electropositive electronic distribution.<sup>23</sup> Thus, the low antifungal activity of these peptides could be attributed to the inadequate balance between cationic and hydrophobic residues in their sequences. It should be noted that a determinant role for the W residues in the membrane translocation of peptides has been proposed.<sup>24</sup> The mutation of both tryptophans in penetratin was found to abolish internalization.<sup>25</sup> Based on these observations, in the present new series we gradually reduced the number of cationic residues, thereby increasing the number of hydrophobic amino acids. This way, we designed a set of nine

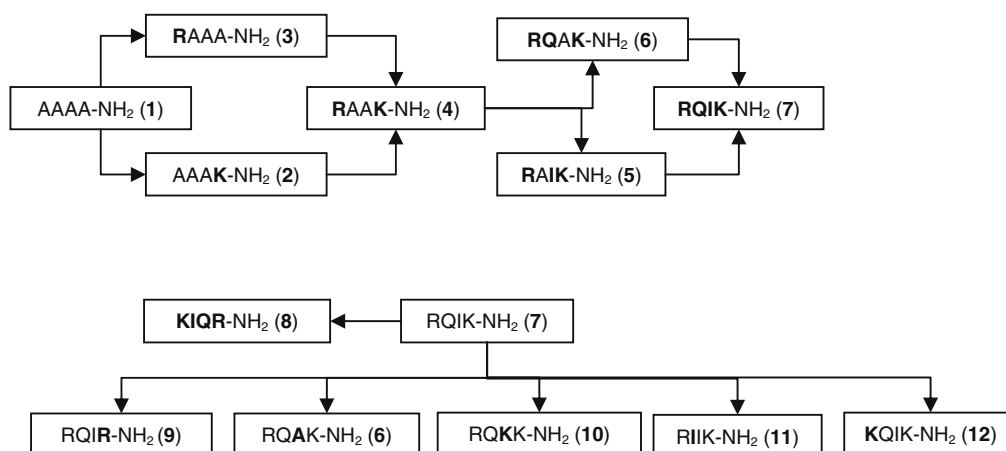


Figure 1. Systematic sequential changes performed on tetrapeptides. Starting from AAAAA-NH<sub>2</sub> 12 different peptides were obtained changing one residue step by step.

**Table 1**  
Antifungal activity (% inhibition) of peptides **1–12** against *Cryptococcus neoformans* ATCC 32264

Peptide	Sequence	MICs						
		200 $\mu$ M	100 $\mu$ M	50 $\mu$ M	25 $\mu$ M	12.5 $\mu$ M	6.25 $\mu$ M	3.125 $\mu$ M
<b>1</b>	AAAA-NH <sub>2</sub>	24.96 $\pm$ 11.23	24.55 $\pm$ 12.74	17.34 $\pm$ 11.7	20.36 $\pm$ 3.78	11.77 $\pm$ 4.35	12.37 $\pm$ 3.9	5.93 $\pm$ 0.19
<b>2</b>	AAAK-NH <sub>2</sub>	70.57 $\pm$ 2.01	61.97 $\pm$ 7.95	57.94 $\pm$ 12.1	42.98 $\pm$ 7.78	31.06 $\pm$ 4.41	0	0
<b>3</b>	RAAA-NH <sub>2</sub>	38.40 $\pm$ 6.1	8.45 $\pm$ 1.15	8.43 $\pm$ 0.1	8.90 $\pm$ 0.47	6.08 $\pm$ 0.32	4.96 $\pm$ 0.49	0
<b>4</b>	RAAK-NH <sub>2</sub>	78.60 $\pm$ 1.69	69.72 $\pm$ 4.81	67.54 $\pm$ 5.18	39.08 $\pm$ 4.52	26.33 $\pm$ 3.79	14.07 $\pm$ 1.54	0
<b>5</b>	RAIK-NH <sub>2</sub>	34.61 $\pm$ 4.13	29.13 $\pm$ 6.42	0	0	0	0	0
<b>6</b>	RQAK-NH <sub>2</sub>	0	0	0	0	0	0	0
<b>7</b>	RQIK-NH <sub>2</sub>	55.44 $\pm$ 12.5	36.63 $\pm$ 1.84	18.37 $\pm$ 2.59	17.54 $\pm$ 2.17	11.20 $\pm$ 2.16	19.94 $\pm$ 1.84	12.15 $\pm$ 3.22
<b>8</b>	KIQR-NH <sub>2</sub>	47.65 $\pm$ 2.15	44.09 $\pm$ 2.34	30.86 $\pm$ 2.11	26.91 $\pm$ 4.28	25.14 $\pm$ 2.32	21.22 $\pm$ 7.99	20.93 $\pm$ 7.09
<b>9</b>	RQIR-NH <sub>2</sub>	65.65 $\pm$ 6.8	40.17 $\pm$ 6.5	18.82 $\pm$ 1.8	19.27 $\pm$ 4.4	3.34 $\pm$ 0.5	0	0
<b>10</b>	RQKK-NH <sub>2</sub> <sup>a</sup>	100 $\pm$ 1.2	100 $\pm$ 4	92.00 $\pm$ 3.6	62.00 $\pm$ 7.4	32.00 $\pm$ 2.3	0	0
<b>11</b>	RIIK-NH <sub>2</sub>	42.00 $\pm$ 7.35	39.74 $\pm$ 11.7	11.46 $\pm$ 1.18	20.94 $\pm$ 2.26	12.64 $\pm$ 1.53	14.53 $\pm$ 6.04	8.74 $\pm$ 1.21
<b>12</b>	KQIK-NH <sub>2</sub>	3.72 $\pm$ 0.41	0	0	0	0	0	0
Amph. B <sup>b</sup>		100	100	100	100	100	100	100
Ket <sup>c</sup>		100	100	100	100	100	100	100

<sup>a</sup> Previously reported in Ref. 23.

<sup>b</sup> Amphotericin B.

<sup>c</sup> Ketoconazole.

small-size peptides possessing sequences somewhat different, but structurally much related among them (compounds **18–26**, Table 2). Peptides **18** and **19** were designed as to maintain the stereo-electronic characteristics of the first four and the last three amino acids of penetratin. Note that the first four amino acids of these peptides possess as features cationic–polar–hydrophobic–cationic amino acids; whereas the last three amino acids are hydrophobic–cationic–cationic. Peptides **18** and **19** possess five cationic residues (R1, K4, K5, R10, and R11 in the case of **18** and R1, R4, R5, R10, and R11 for **19**). Peptide **20** keeps the first four amino acids of peptide **19** but the last two residues were replaced by hydrophobic amino acids (W10 and W11) diminishing the number of cationic residues from five to three. In peptides **21** and **22** the number of cationic residues was further reduced to two and one, respectively. In peptide **23** we retained the electronic characteristics of the first four amino acids, but the total number of amino acids was reduced from 11 to 9. Peptides **24** and **25** are nonapeptides structurally related to **23**, however in these compounds the number of cationic residues was reduced to two and only one, respectively. The set of peptides under study was completed with peptide **26**. It should be noted that the sequence of this peptide corresponds to the last eight residues of penetratin.

In order to decide which of these peptides was preferred to be synthesized and tested we performed a conformational and electronic analysis on these compounds trying to determine pharmacophoric patterns comparable to that previously obtained for penetratin.

## 2.1. Conformational analysis

As was previously mentioned,<sup>23</sup> linear peptides are highly flexible and to determine their biologically relevant conformations is therefore complex. It is necessary to perform an exhaustive conformational analysis for these structures and in the present study we thus carried out calculations using EDMC computations,<sup>26,27</sup> which previously turned out to be successful for penetratin and its derivatives.<sup>23</sup>

The EDMC results are summarized in Table 3 and more details are given in Tables 1S–9S in Supplementary data. Calculations yielded a large set of conformational families for each peptide studied. The total number of conformations generated for each peptide varied between 104,810 and 130,215, and the number of those accepted was 5000 for all cases. In the clustering procedure, an RMSD (root mean square deviation) of 0.75 Å and a cutoff of

30 kcal mol<sup>-1</sup> were used. The number of families after clustering varied between 238 and 463. The total number of families accepted possessing a relative population higher than 0.20% varied between 7 and 22. The relative populations summed up to ca. 88% of all conformations in each case (see % *P* in Table 3). All low-energy conformers of these peptides were then compared to each other. The comparison involved the spatial arrangements, relative energy and populations.

It is interesting to note that the energetically and populated preferred families comprise more than 61% of the entire population for each peptide (see Table 3, last column). Thus, these families adopting an  $\alpha$ -helix structure are the most representative forms for these peptides. This conformation is characterized by stabilizing hydrogen bonds between the carbonylic oxygen (residue *i*) and the NH group (residue *i* + 4). The first and the last residues do not present a stable structure in any of the cases. A spatial image of this conformation is shown for peptide **18** in Figure 2.

The second most populated family obtained for peptides **18–20** do not demonstrate a significant percentage of population (0.44%, 2.2%, and 0.76%, respectively). The second most populated family obtained for peptides **21–26** displayed a percentage of population ranging between 4.98% and 9.18% possessing bend, turn forms or not showing any stable structures. In general these conformations showed an energy gap ranging between 4.29 and 9.50 kcal mol<sup>-1</sup> above their respective global minimum. These results suggest that  $\alpha$ -helix forms are the highly preferred conformations for these peptides.

To better characterize the peptide spatial orientations, we plotted Edmundson wheel representations of peptides **18–26** (Fig. 3). The wheel representations obtained for peptides **18**, **19**, and **23** were very similar. They display two clearly differentiated faces: the ‘charged face’ (denoted in dash blue line in Fig. 3) and a ‘non-charged face’ (depicted in full green line). The first face identifies residues R1, K4, K5, and R11 (in peptide **18**); R1, R4, R5, and R11 (in peptide **19**) and R1, R4, and R5 in peptide **23**, as those accounting for the mutual coulombic binding. The first three residues are located on the same side of the helical peptide and we call it the ‘charged face’. These positively charged residues are able to produce salt bridges with the lipids. The non-charged face is formed by four hydrophobic (W3, W6, W7, and W9 in peptide **18**) and one polar residue (Q2). Considering the general electronic distribution, these representations resemble very well those previously reported for penetratin.<sup>23</sup> It is clear however, that both faces in these small-size peptides are substantially reduced in

**Table 2**  
Antifungal activity (% inhibition) of peptides **13–26** against *Candida albicans* ATCC 10231 and *Cryptococcus neoformans* ATCC 32264

Peptide	Sequence	<i>Candida albicans</i>					<i>Cryptococcus neoformans</i>				
		200 $\mu$ M	100 $\mu$ M	50 $\mu$ M	25 $\mu$ M	12.5 $\mu$ M	200 $\mu$ M	100 $\mu$ M	50 $\mu$ M	25 $\mu$ M	12.5 $\mu$ M
<b>13<sup>a</sup></b>	RQIKWFQNRIRMKWKK-NH <sub>2</sub>	100 ± 0.2	100 ± 0.6	95 ± 1.2	91 ± 1.6	4 ± 0.1	100 ± 0.1	100 ± 0	100 ± 0	100 ± 0.2	90 ± 2.3
<b>14<sup>a</sup></b>	RKWRKWK-NH <sub>2</sub>	100 ± 0.08	76 ± 0.97	58 ± 0.71	40 ± 1.75	15 ± 1.0	99 ± 1.68	68 ± 21.22	14 ± 1.32	16 ± 1.78	0
<b>15<sup>a</sup></b>	RKFRKFKK-NH <sub>2</sub>	61 ± 1.16	44 ± 7.0	33 ± 7.42	23 ± 3.79	0	73 ± 1.51	11 ± 3.92	13 ± 2.32	9 ± 3.8	0
<b>16<sup>a</sup></b>	RKRRKWK-NH <sub>2</sub>	29 ± 1.05	13 ± 0.55	0	0	0	100 ± 0.36	33 ± 4.79	11 ± 4.35	6 ± 2.14	0
<b>17<sup>a</sup></b>	RKRRKWK-NH <sub>2</sub>	43 ± 4.96	12 ± 0.4	0	0	0	60 ± 2.94	14 ± 2.09	19 ± 6.73	10 ± 2.89	0
<b>18</b>	RQWKQWQVRR-NH <sub>2</sub>	100 ± 0	100 ± 0	100 ± 0	67.90 ± 5	35.68 ± 3.28	100 ± 0	100 ± 0	100 ± 0	100 ± 0	66.25 ± 6.31
<b>19</b>	RQRRWQVRR-NH <sub>2</sub>	100 ± 0	100 ± 0	100 ± 0	46.56 ± 0.33	22.89 ± 0.77	100 ± 0	100 ± 0	100 ± 0	100 ± 0	51.17 ± 7.07
<b>20</b>	RQRRWQVRR-NH <sub>2</sub>	n.t.	n.t.	n.t.	n.t.	n.t.	n.t.	n.t.	n.t.	n.t.	n.t.
<b>21</b>	RQIKWQVRR-NH <sub>2</sub>	n.t.	n.t.	n.t.	n.t.	n.t.	n.t.	n.t.	n.t.	n.t.	n.t.
<b>22</b>	RQVWVQVRR-NH <sub>2</sub>	n.t.	n.t.	n.t.	n.t.	n.t.	n.t.	n.t.	n.t.	n.t.	n.t.
<b>23</b>	RQRRWQVRR-NH <sub>2</sub>	100 ± 0	100 ± 0	100 ± 0	50.70 ± 2.04	19.09 ± 3.85	100 ± 0	100 ± 0	100 ± 0	100 ± 0	83.35 ± 5.66
<b>24</b>	RQRRWQVRR-NH <sub>2</sub>	n.t.	n.t.	n.t.	n.t.	n.t.	n.t.	n.t.	n.t.	n.t.	n.t.
<b>25</b>	RQVWVQVRR-NH <sub>2</sub>	n.t.	n.t.	n.t.	n.t.	n.t.	n.t.	n.t.	n.t.	n.t.	n.t.
<b>26</b>	NRRMKWKK-NH <sub>2</sub>	10.99 ± 1.4	4.59 ± 12.64	0	0	0	63.63 ± 1.61	34.76 ± 2.31	23.29 ± 1.41	6.71 ± 2.48	6.64 ± 0.69
Amph. B <sup>b</sup>		100	100	100	100	100	100	100	100	100	100
Ket <sup>c</sup>		100	100	100	100	100	100	100	100	100	100

n.t., not tested.

The main mutation performed in the peptide sequences and the percentage of inhibition higher than 60, are denoted in bold.

<sup>a</sup> Previously reported in Ref. 23.<sup>b</sup> Amphoterin B.<sup>c</sup> Ketoconazole.

comparison to penetratin as function of their smaller size. The wheel representation obtained for peptide **20** displays a somewhat reduced cationic face in comparison to **19**, however the general distribution is still comparable. In contrast, the wheel representations obtained for peptides **21**, **22**, **24**, and **25** reveals a dominant hydrophobic face and a markedly reduced cationic zone. This difference can be appreciated observing the larger full green lines obtained for these representations (Fig. 3). Peptide **26** has a completely different wheel representation compared to the rest of the peptides previously analyzed. This peptide possesses four small intercalated faces, two of them with cationic characteristics and the other two showing hydrophobic zones.

Next we performed a detailed electronic study of peptides **18–26** obtained using quantum mechanics calculations (RHF/6-31G).

## 2.2. Molecular electrostatic potentials (MEPs)

The electronic study of the peptides **18–26** was performed using MEPs.<sup>28</sup> MEPs have been shown to provide reliable information, both on the interaction sites of molecules with point charges and on the comparative reactivities of those sites.<sup>28,29</sup> More positive potentials reflect nucleus predominance, while less positive values represent rearrangements of electronic charges and lone pairs of electrons. The fundamental application of this study is the analysis of non-covalent interactions, mainly by investigating the electronic distribution in the molecule. Thus, this methodology was used to evaluate the electronic distribution around the molecular surface of the peptides here reported.

We evaluated and plotted the MEPs of peptides **18–26** showing only the most representative results in Figures 4–7, whereas the rest are included in Supplementary data. To better appreciate the electronic behavior of peptide **18** (Fig. 4), and considering that two different faces were signaled in Figure 3, we present the MEPs of this peptide showing both faces. Figure 4a gives the ‘charged face’ (CF) characterized by the presence of four cationic residues (R1, K4, K5, and R11). Tryptophan fluorescence studies previously reported for penetratin showed the importance of peptide positively charged residues for the initial binding to negatively charged vesicles, since double R/K→A mutations involving the residues K4/R10/R11 significantly decreased the binding affinity.<sup>30</sup> The MEPs of **18** suggests that some of the above mentioned residues (R1, K4, K5, and R11) could be responsible for the initial binding. The main positive potentials ( $V(r)$  ranging from 0.73 to 0.48 e au<sup>-3</sup>) are concentrated on the charged face; however it should be noted that the residue R10 is located in the hydrophobic face. Thus, this cationic residue appears to be strategically located in the middle of the non-charged face. Figure 4b displays the hydrophobic face of **18** showing four hydrophobic residues (W9, W6, W3, and W7) and a polar one (Q2). It appears that a kind of pi-stacking cluster through W3/W6/W9 takes place in this portion of **18**. Also peptide **18** contains two polar residues (Q2 and Q8) which are located one on each face. The MEPs displayed for peptide **19** (Fig. 1S in Supplementary data) is very similar to that obtained for **18**.

The MEPs of peptides **20–22** (Figs. 2S, 3S and 5, respectively) revealed significant differences compared to those of peptides **18** and **19**. They show an increasing hydrophobic zone and a systematically diminished cationic face characterized by an extended yellow and orange zone pointing to a ‘too hydrophobic’ distribution.

Although peptide **23** is smaller in size than peptides **18** and **19** the general electronic distribution of this nonapeptide is closely related to those of peptides **18** and **19** showing two clearly differentiated faces, the cationic (Fig. 6a) and the hydrophobic (Fig. 6b). In contrast the MEPs calculated for peptides **24** and **25** (Fig. 4S and 7) have an electronic distribution rather similar to those of peptides **21** and **22**.

**Table 3**  
Selected conformational search and clustering results for peptides **18–26** optimized at the EDMC/SRFOPT/ECCEP/3 level of theory

Peptide	Generated <sup>a</sup>				Accepted <sup>b</sup>				#F	#F <sub>0.2%</sub>	% P	% PP
	Electrostatical	Random	Thermal	Total	Electrostatical	Random	Thermal	Total				
18	8558	114,205	456	123,219	1229	3475	296	5000	379	7	90.10	88.16
19	9063	120,668	484	130,215	1413	3298	289	5000	364	8	90.26	84.66
20	8694	117,218	443	126,355	1122	3611	267	5000	360	13	90.48	84.76
21	7967	110,585	470	119,022	947	3785	268	5000	379	19	90.20	61.70
22	8474	116,864	544	125,882	1040	3648	312	5000	463	18	88.38	64.42
23	8031	106,448	300	114,779	1211	3574	215	5000	333	22	91.02	66.90
24	8127	108,917	348	117,392	1162	3592	246	5000	343	18	91.20	65.34
25	8247	111,489	445	120,181	878	3802	320	5000	410	15	90.10	72.38
26	7070	97,498	242	104,810	946	3859	195	5000	238	15	94.04	75.86

#F represents the total number of conformational families as result of the clustering run.

#F<sub>0.2%</sub> represents the number of conformational families with population above 0.2%.

% P represents the sum of the percent relative population of #F<sub>0.2%</sub>.

% PP percent relative population for the most populated and energetically preferred family.

<sup>a</sup> Number of conformations generated electrostatically, randomly and thermally during the conformational search.

<sup>b</sup> Number of conformations accepted from those generated electrostatically, randomly and thermally during the conformational search.

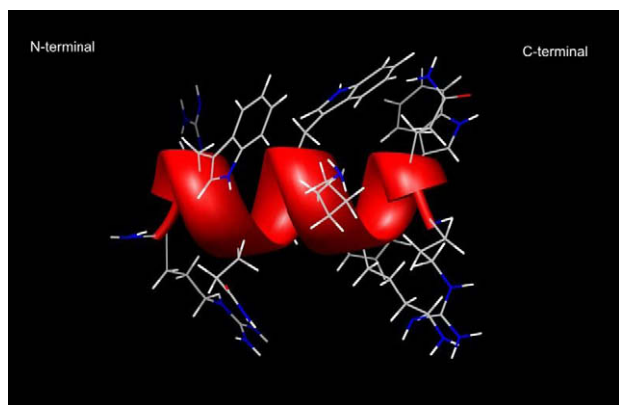


**Figure 2.** Spatial view of the global minimum ( $\alpha$ -helix structure) obtained for peptide **18**.

In agreement with the different wheel representation obtained for peptide **26**, this peptide presented a completely different electronic distribution as well. The electronic study suggested that peptides **18**, **19**, and **23** have an electronic distribution in accordance with the previously proposed pharmacophoric pattern. This pattern suggests a particular combination of cationic and hydrophobic residues adopting a definite spatial ordering which appears to be the key parameter for the transition from hydrophilic to hydrophobic phase. In contrast peptides **21**, **22**, **24**, and **25** displayed a different electronic distribution which might be considered 'too hydrophobic' with respect to the more balanced electronic distributions.

### 2.3. Synthesis and antifungal activity

On the basis of the results obtained with the conformational and electronic studies we synthesized and tested peptides **18**, **19**, and **23**. These peptides were thoroughly selected on the basis of their conformational and electronic behavior being closely related to that previously reported for penetratin.<sup>23</sup> In addition, we synthesized and tested peptide **26** presenting an entirely different peptide spatial orientation and also a different electronic behavior not agreeing with the proposed pharmacophoric pattern and thus could act as a negative control.

The Minimum Inhibitory Concentrations (MIC) of peptide **1–26** was determined in the range of concentrations from 200 to 3.125  $\mu$ M with the standardized microbroth dilution method

M-27 A2 for yeasts recommended by the Clinical and Laboratory Standards Institute (CLSI, formerly National Committee for Clinical and Laboratory Standards NCCLS).<sup>31</sup> At each concentration tested (200, 100, 50, 25, 12.5, 6.25, and 3.125  $\mu$ M) the % of inhibition displayed by each peptide was determined. Compounds producing no inhibition of fungal growth at 200  $\mu$ M were considered inactive. Table 2 gives the antifungal activity obtained for peptides **18**, **19**, **23**, and **26** against *C. albicans* and *C. neoformans*. Results showed that the first three peptides displayed a significant antifungal activity against both fungi tested being *C. neoformans* the most susceptible species. Peptides **18**, **19**, and **23** inhibit 100% (MIC<sub>100</sub>) the growth of *C. neoformans* at 25  $\mu$ M, but interestingly enough, they produced 66%, 51%, and 83% inhibition, respectively, at 12.5  $\mu$ M. These results signify that the three compounds possess MIC<sub>50</sub> (concentration at which the compounds produce 50% inhibition)  $\leq$  12.5  $\mu$ M and compound **23** displayed a MIC<sub>80</sub>  $\leq$  12.5  $\mu$ M. The application of a less stringent end-point such as MIC<sub>80</sub> and MIC<sub>50</sub> has been recommended by CLSI because it showed to consistently represent the in vitro activity of compounds and many times provide a better correlation with other measurements of antifungal activity. So, the fact that these three peptides possess very low MIC<sub>80</sub> and MIC<sub>50</sub> values against *C. neoformans* is very interesting. This species remains an important life-threatening complication for immunocompromised hosts being the main cause of fatal meningoencephalitis in AIDS patients and producing fatal cryptococcosis in patients who have undergone transplantation of solid organs. Therefore, new compounds acting against this fungus are highly welcome.

In turn, compounds **18**, **19**, and **23** also inhibit *C. albicans*, with MIC<sub>100</sub> = 50  $\mu$ M and MIC<sub>50</sub>  $\leq$  25  $\mu$ M. This is also an interesting finding because candidiasis is the fourth most common nosocomial blood stream infection, representing more than 60% of all isolates from clinical infections.<sup>32</sup>

It should be noted that the antifungal effects obtained for these small-size peptides are slightly better to those previously reported for penetratin which displayed a MIC<sub>50</sub> between 12.5 and 25  $\mu$ M.<sup>23</sup> In contrast and as we expected, peptide **26** was devoid of any significant antifungal activity. These experimental results clearly support our theoretical calculations obtained from molecular and quantum mechanics computations. In addition, these theoretical and experimental results are an additional support for the pharmacophoric pattern previously proposed for penetratin and its derivatives.<sup>23</sup>

At this stage of our studies, some general conclusions may be drawn. Peptides **14–17** revealed only a marginal antifungal effect (peptide **14**) or were inactive. These results indicate that such

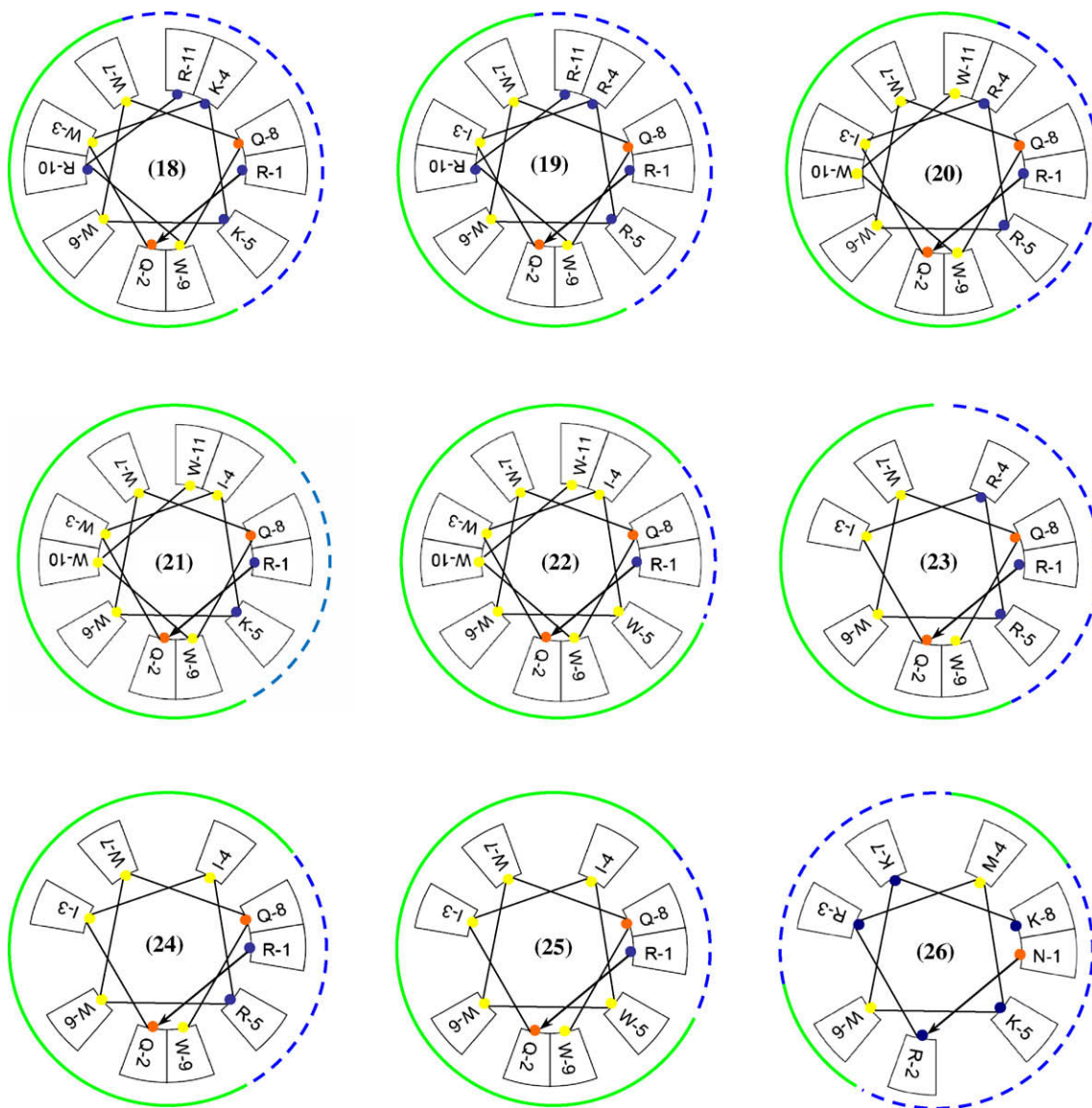


**Figure 3.** Edmundson wheel representations of peptides **18–26**. The number in the center of the wheel corresponds to the peptide number. The ‘charged’ and ‘non-charged’ faces are shown in blue dashed lines and full green lines, respectively. Positively charged amino acids are denoted with blue dots, the polar ones with orange, and the hydrophobic ones with yellow.

cationic peptides could not be sufficiently hydrophobic to penetrate deeply into phospholipid model membranes.<sup>33,34</sup> Therefore, charge neutralization is required for a deeper insertion of the peptide into the hydrophobic core of the membrane. The non-charged face possessing at least one cationic or polar residue among the hydrophobic ones observed in the MEPs of peptides **18**, **19**, and **23** appears to be operative in this sense. Previously reported MD simulations indicated that the aromatic residues do not contribute to the initial binding, but rather to the subsequent insertion of penetratin between the bilayer head groups, when they shield the peptide from the aqueous phase.<sup>35</sup> The importance of hydrophobic residues seems to be crucial for the antifungal activity of these small-size peptides as well. However, our results indicate that a balanced electronic distribution (not ‘too cationic’ and not ‘too hydrophobic’) is necessary to produce the antifungal effect.

In general the toxicity of the antifungal agents is a critical aspect for their usefulness and limitations. Thus, in addition to the antifungal evaluation, the acute toxic effect of compounds **18**, **19**,

and **23** were evaluated using a toxicity test on fish which has been previously successfully used by our group on other antifungal compounds.<sup>36–38</sup> Our results indicated that none of these peptides displayed acute toxicity (measured as fish mortality during 96 h) at 13 µg/ml (Table S10 in Supplementary data). Although, these are preliminary results they give a promising feature about the low acute toxicity of these peptides.

In terms of bioavailability, stability, and pharmacokinetics, most peptides are as bad as proteins and, in general do not make good drugs unless chemical modifications are performed on their structure. It is clear that in general peptides possess significant limitations to be used directly as drugs; however many of these peptides are excellent starting structures to develop new drugs (generally as peptidomimetic compounds) with novel mechanisms of action and therefore developing new effective and safer therapeutic agents. It is clear that these results must be considered as preliminary results in the long way of the design of antifungal leads; however they allowed the identification of a promising 3D pharmacophore for these compounds.

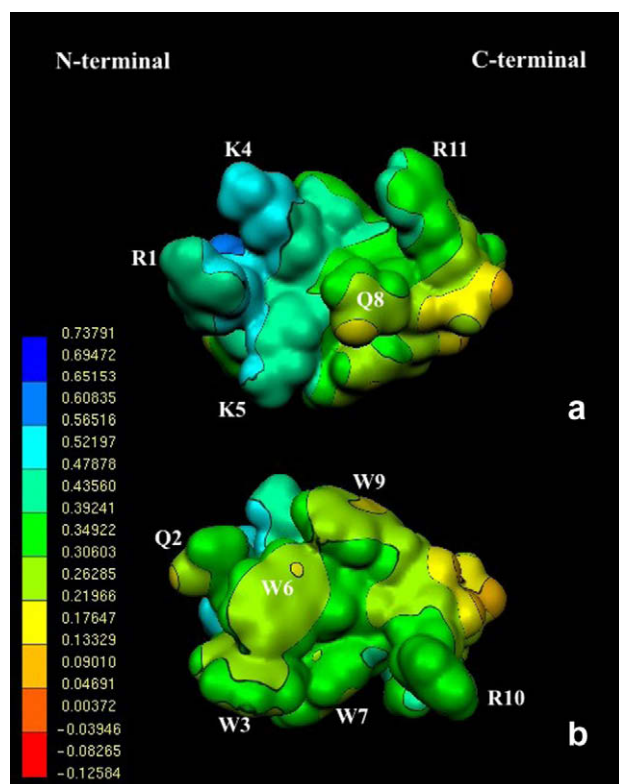


**Figure 4.** Electrostatic potential-encoded electron density surfaces of peptide 18. (a) 'Charged face' and (b) 'non-charged face'. The surfaces were generated with GAUSSIAN 03 using RHF/6-31G single point calculations. The coloring represents electrostatic potential with red indicating the strongest attraction to a positive point charge and blue indicating the strongest repulsion. The electrostatic potential is the energy of interaction of the positive point charge with the nuclei and electrons of a molecule. It provides a representative measure of overall molecular charge distribution. The color-coded is shown at the left.

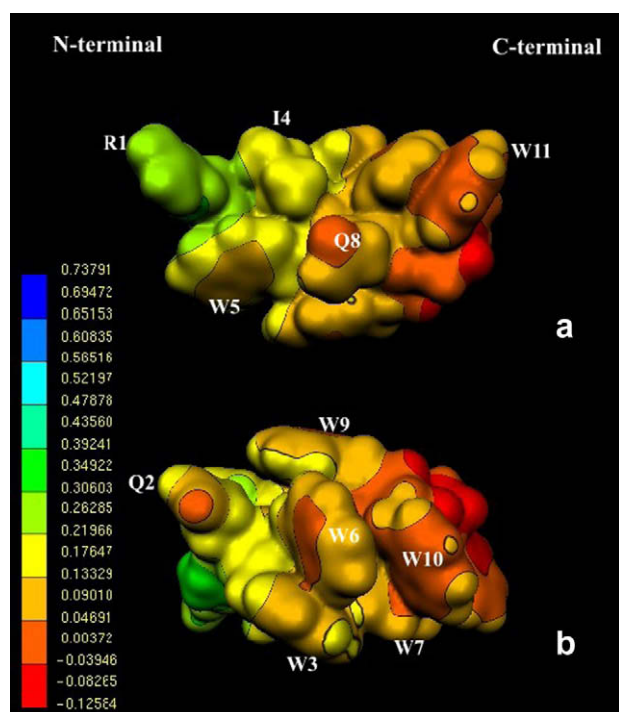


**Figure 5.** Electrostatic potential-encoded electron density surfaces of peptide 22. (a) 'Charged face' and (b) 'non-charged face'.

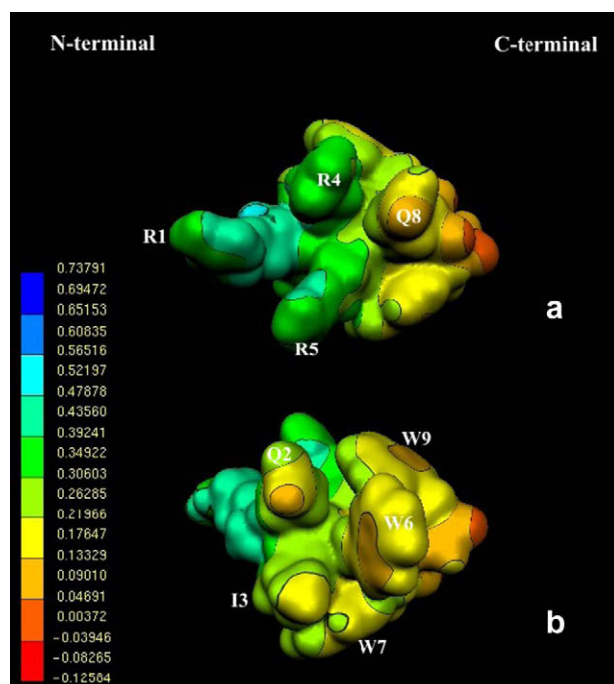


**Figure 6.** Electrostatic potential-encoded electron density surfaces of peptide 23. (a) 'Charged face' and (b) 'non-charged face'.

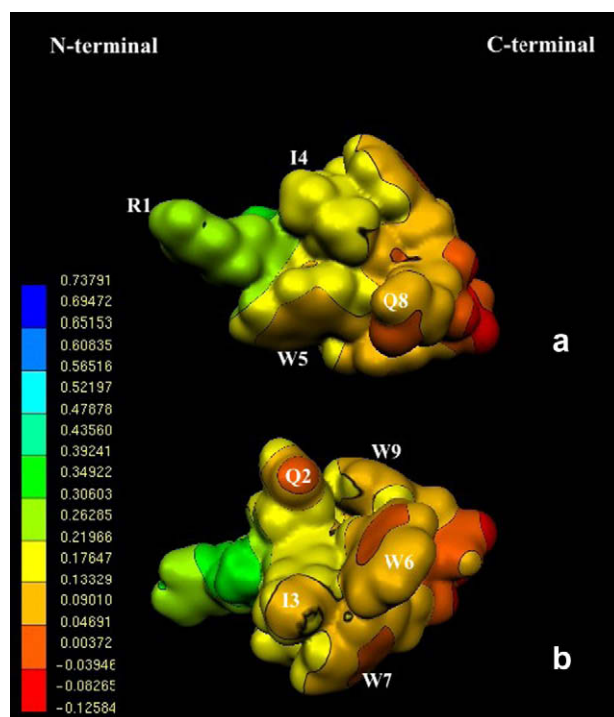


**Figure 7.** Electrostatic potential-encoded electron density surfaces of peptide 25. (a) 'Charged face' and (b) 'non-charged face'.

Finally, it is important to highlight that the mechanism of action of these peptides has not been determined yet. Nevertheless, as a general feature, antimicrobial cationic peptides possess a relatively non-specific mechanism of action by either acting through a detergent-like disruption of the bacterial or fungal cell membrane or by

the formation of transient transmembrane pores.<sup>39,40</sup> Therefore, due to their cationic and amphipathic structural characteristics, it is likely to be that these peptides possess the features of the general mechanisms of action of antimicrobial cationic peptides. However, we have not yet definitive results about the possible molecular mechanism for these peptides. Different bioassays are being carried out in our laboratories in order to obtain sufficient information regarding this matter.

### 3. Conclusions

In the present paper, we report the design, synthesis, and antifungal effects of small-size peptides. On the basis of a detailed conformational and electronic study performed on a series of compounds, we obtained a new series of small-size peptides containing 9 and 11 amino acids showing potential antifungal effects. Among the peptides tested, RQWKKWWQWRR-NH<sub>2</sub>, RQIRWWQWRR-NH<sub>2</sub>, and RQIRWWQW-NH<sub>2</sub> displayed the most potent inhibitory effect against both *C. neoformans* and *C. albicans*.

A comprehensive conformational and electronic study performed using theoretical calculations provided an additional support for the pharmacophoric pattern previously reported for penetratin and its derivatives. This pattern suggests a particular combination of cationic and hydrophobic residues adopting a definite spatial ordering which appears to be the key parameter for the membrane transition from hydrophilic to hydrophobic phase. This transition proved to be a necessary step to produce the antifungal activity. We conclude that the present results contribute to the understanding of the minimal structural requirements for the antifungal effects of these selected peptides and the design of novel structurally related agents. Thus, we have identified a structural template that can serve as a 3D pharmacophore for the design of new effective antifungal compounds particularly against *C. albicans* and *C. neoformans*.

## 4. Experimental section

### 4.1. Synthetic methods

Solid phase synthesis of the peptides was carried out manually on a *p*-methyl benzhydrylamine resin (1 g MBHA, 0.14 mmol/g) with standard methodology using Boc-strategy. Side chain protecting groups were as follows: Arg(Tos), His(Tos), Lys(2Cl-Z), Cys(MbzI), Tyr(2-Br-Z). All protected amino acids were coupled in CH<sub>2</sub>Cl<sub>2</sub> (5 ml) using DCC (2.5 equiv) and HOBT (2.5 equiv) until completion (3 h) judged by Kaiser et al.<sup>41</sup> ninhydrin test. After coupling of the appropriate amino acid, Boc deprotection was effected by use of TFA/CH<sub>2</sub>Cl<sub>2</sub> (1:1, 5 ml) for 5 min first then repeated for 25 min. Following neutralization with 10% TEA/CH<sub>2</sub>Cl<sub>2</sub> three times (5–5 ml of each), the synthetic cycle was repeated to assemble the resin-bond protected peptide. The peptides were cleaved from the resin with simultaneous side chain deprotection by acidolysis with anhydrous hydrogen fluoride (5 ml) containing 2% anisole, 8% dimethyl sulfide and indole at 5 °C for 45 min. The crude peptides were dissolved in aqueous acetic acid and lyophilized. Preparative and analytical HPLC of the crude and the purified peptides were performed on an LKB Bromma apparatus (for preparative HPLC, column: Lichrosorb RP C18, 7 μm, 250 × 16 mm; gradient elution: 30–100%, 70 min; mobile phase: 80% acetonitrile, 0.1% TFA; flow rate: 4 ml/min, 220 nm, for analytical HPLC, column: Phenomenex Luna 5C18(2), 250 × 4.6 mm; mobile phase: 80% acetonitrile, 0.1% TFA; flow rate: 1.2 ml/min, 220 nm, ESI-MS: Finnigan TSQ 7000).

HPLC data of the synthesized peptides.

	Retention factor (min)	Gradient elution (%)
AAAANH <sub>2</sub> ( <b>1</b> )	6.124	0–30 (15 min)
AAAK-NH <sub>2</sub> ( <b>2</b> )	3.468	5–20 (15 min)
RAAA-NH <sub>2</sub> ( <b>3</b> )	8.037	0–15 (15 min)
RAAK-NH <sub>2</sub> ( <b>4</b> )	3.750	5–20 (15 min)
RAIK-NH <sub>2</sub> ( <b>5</b> )	8.192	5–20 (15 min)
RQAK-NH <sub>2</sub> ( <b>6</b> )	3.579	5–20 (15 min)
RQIK-NH <sub>2</sub> ( <b>7</b> )	9.550	0–40 (20 min)
KIQR-NH <sub>2</sub> ( <b>8</b> )	6.674	5–30 (15 min)
RQIR-NH <sub>2</sub> ( <b>9</b> )	8.463	5–30 (15 min)
RIIK-NH <sub>2</sub> ( <b>11</b> )	8.507	5–80 (25 min)
KQIK-NH <sub>2</sub> ( <b>12</b> )	9.607	0–20 (20 min)
RQWKKWWQWRR-NH <sub>2</sub> ( <b>18</b> )	6.334*	27–42 (15 min)
RQIRWWQWRR-NH <sub>2</sub> ( <b>19</b> )	8.046*	24–39 (15 min)
RQIRWWQW-NH <sub>2</sub> ( <b>23</b> )	6.182	32–47 (15 min)
NRMRKWK-NH <sub>2</sub> ( <b>26</b> )	6.117	14–29 (15 min)

\*Flow rate: 1 ml/min.

Only the MS data obtained for the most representative peptides are reported here. The instrument for ESI-MS was Finnigan TSQ 7000 and the data are as follows: RQWKKWWQWRR-NH<sub>2</sub> (**18**) 1743.8 (M+1), 872.3 (M/2+1), 581.8 (M/3+1), 436.5 (M/4+1), 349.2 (M/5+1); RQIRWWQWRR-NH<sub>2</sub> (**19**) 1726.9 (M+1), 863.9 (M/2+1), 576 (M/3+1), 432.3 (M/4+1), 345.8 (M/5+1); RQIRWWQW-NH<sub>2</sub> (**23**) 1414.5 (M+1), 707.5 (M/2+1) 472 (M/3+1).

### 4.2. Microorganisms and media

Strains of *C. albicans* and *C. neoformans* from the American Type Culture Collection (ATCC, Rockville, MD, USA) were used. *C. albicans* ATCC 10231, *Candida tropicalis* C 131, and *C. neoformans* ATCC 32264 were grown on Sabouraud-chloramphenicol agar slants for 24 h at 35 °C, maintained on slopes of Sabouraud-dextrose agar (SDA, Oxoid). Inocula of cell suspensions were obtained according to reported procedures and adjusted to 1–5 × 10<sup>3</sup> cells with colony forming units (CFU)/ml.<sup>31</sup>

### 4.3. Antifungal evaluation

The test was performed in 96 wells-microplates. Peptide test wells (PTW) were prepared with stock solutions of each peptide in DMSO (≤2%), diluted with RPMI-1640 to final concentrations 200–3.125 μM. Inoculum suspension (100 μl) was added to each well (final volume in the well = 200 μl). A growth control well (GCW) (containing medium, inoculum, the same amount of DMSO used in PTW, but compound-free) and a sterility control well (SCW) (sample, medium, and sterile water instead of inoculum) were included for each strain tested. Microtiter trays were incubated in a moist, dark chamber at 35 °C, 24 or 48 h for *Candida* spp. or *Cryptococcus* sp., respectively. Microplates were read in a VERSA Max microplate reader (Molecular Devices, Sunnyvale, CA, USA). Amphotericin B (Sigma Chemical Co, St. Louis, MO, USA) was used as positive control (100% inhibition). Tests were performed by duplicate. Reduction of growth for each peptide concentration was calculated as follows: % of inhibition: 100 – (OD<sub>405</sub> PTW – OD<sub>405</sub> SCW)/OD<sub>405</sub> GCW – OD<sub>405</sub> SCW.

#### 4.3.1. Statistical analysis

Data were statistically analyzed by both, one-way analysis of variance and Student's test. A *p* < 0.05 was considered significant.



#### 4.4. Acute toxicity test

Toxic effect of compounds was evaluated using a toxicity test on fish. The static technique recommended by the US Fish and Wildlife Service Columbia National Fisheries Research Laboratory<sup>42</sup> was modified in order to use lower amounts of tested compounds.<sup>36</sup> Fish of the specie *Poecilia reticulata* were born and grown in our laboratory until they reached a size of 0.7–1 cm (15 days old). In the toxicity test, 10 specimens were exposed to each of the concentration tested per drug in 2 l wide-mouthed jars containing the test solutions. Aqueous stock solutions of pure compounds diluted in DMSO were prepared and added to test chambers to get the final concentrations. The test began upon initial exposure to the peptides and continued for 96 h. The number of dead organisms in each test chamber was recorded and the dead organisms were removed every 24 h; general observations on the conditions of tested organisms were also recorded at this time; however the percentage of mortality was recorded at 96 h. Each experience was performed two times with three replicates each. We chose this technique because it is fast, economic, and easy to reproduce. This assay has been previously used by our group testing the toxicity of synthetic and natural compounds.<sup>36–38</sup> The species *P. reticulata* has been previously used in acute toxicity test.<sup>43</sup>

#### 4.5. Computational methods

##### 4.5.1. EDMC calculations

The conformational space was explored using the method previously employed by Liwo et al.<sup>44</sup> that included the electrostatically driven Monte Carlo (EDMC) method<sup>26,45</sup> implemented in the ECEPPAK<sup>46</sup> package. Conformational energy was evaluated using the ECEPP/3 force field.<sup>27</sup> Hydration energy was evaluated using a hydration-shell model with a solvent sphere radius of 1.4 Å and atomic hydration parameters that have been optimized using non-peptide data (SRFOPT).<sup>47,48</sup> In order to explore the conformational space extensively, 10 different runs were carried out, each of them with a different random number. Therefore, a total of 5000 accepted conformations were collected. Each EDMC run was terminated after 500 energy-minimized conformations had been accepted. The parameters controlling the runs were the following: a temperature of 298.15 K for the simulations; a temperature jump of 50,000 K, and the maximum number of allowed repetitions of the same minimum was 50. The maximum number of electrostatically predicted conformations per iteration was 400; the maximum number of random-generated conformations per iteration was 100; the fraction of random/electrostatically predicted conformations was 0.30. The maximum number of steps at one increased temperature was 20; and the maximum number of rejected conformations until a temperature jump was executed was 100. Only *trans* peptide bonds ( $\omega \cong 180^\circ$ ) were considered. All accepted conformations were then clustered into families using the program ANALYZE<sup>46</sup> by applying the minimal-tree clustering algorithm for separation, using backbone atoms, energy threshold of 30 kcal mol<sup>-1</sup>, and RMSD of 0.75 Å as separation criteria. This clustering step allows a substantial reduction of the number of conformations and the elimination of repetitions. A more detailed description of the procedure used here is given in Section 4.4 Computational Methods of Ref. 23.

##### 4.5.2. Molecular electrostatic potentials

Quantum mechanics calculations were carried out using the GAUSSIAN 03 program.<sup>49</sup> We use the most populated conformations of peptide 18–26 obtained from EDMC calculations. Subsequently, single point *ab initio* (RHF/6-31G) calculations were carried out. The electronic study was carried out using molecular electrostatic potentials (MEPs).<sup>28</sup> These MEPs were calculated using RHF/6-31G

wave functions and MEPs graphical presentations were created using the MOLEKEL program.<sup>50</sup>

#### Acknowledgements

This work is part of the Hungarian–Argentine Intergovernmental S&T Cooperation Programme. This research was partially supported by grants from Universidad Nacional de San Luis and it is part of the Iberoamerican Project X.7 PIBEFUN (Search and development of new antifungal part of the Iberoamerican Program of Science and Technology for the Development (CYTED)). R.D.E. is a member of the CONICET (Argentina) staff.

#### Supplementary data

Supplementary data associated with this article can be found, in the online version, at doi:10.1016/j.bmc.2009.11.009.

#### References and notes

- Walsh, T. J.; Groll, A.; Hiemenz, J.; Fleming, R.; Roilides, E.; Anaissie, E. *Clin. Microbiol. Infect.* **2004**, *10*, 48.
- Georgopapadakou, N.; Tkacz, J. *Trends Microbiol.* **1995**, *3*, 98.
- Nagiec, M.; Nagiec, E.; Baltisberger, J.; Wells, G.; Lester, R.; Dickson, R. *J. Biol. Chem.* **1997**, *272*, 9809.
- McNeil, M. M.; Nash, S. L.; Hajjeh, R. A.; Phelan, M. A.; Conn, L. A.; Plikaytis, B. D.; Warnock, D. W. *Clin. Infect. Dis.* **2001**, *33*, 641.
- Pfaller, M. A.; Diekema, D. J. *J. Clin. Microbiol. Rev.* **2007**, *20*, 133.
- Pfaller, M. A.; Diekema, D. J. *J. Clin. Microbiol.* **2004**, *42*, 4419.
- Polak, A. *Mycoses* **1999**, *42*, 355.
- Bartroli, J.; Turmo, E.; Algueró, M.; Boncompte, E.; Vericat, M.; Conte, L.; Ramis, J.; Merlos, M.; García-Rafanell, J. *J. Med. Chem.* **1998**, *41*, 1869.
- Epanand, R. M.; Vogel, H. J. *Biochim. Biophys. Acta* **1999**, *1462*, 11.
- Tossi, A.; Sandri, L.; Giangaspero, A. *Biopolymers* **2000**, *55*, 4.
- Hancock, R. E.; Talla, W. T.; Brown, M. H. *Adv. Microb. Physiol.* **1995**, *37*, 135.
- Hancock, R. E. *Lancet* **1997**, *349*, 418.
- Bulet, P.; Stöcklin, R. *Protein Peptide Lett.* **2005**, *12*, 3.
- Park, C. B.; Kim, H. S.; Kim, S. C. *Biochem. Biophys. Res. Commun.* **1998**, *244*, 253.
- Hancock, R. E. W.; Leher, R. *Trends Biotechnol.* **1998**, *16*, 82.
- Bulet, P.; Stöcklin, R. *Protein Peptide Lett.* **2005**, *12*, 3.
- Masman, M. F.; Rodríguez, A. M.; Svetaz, L.; Zacchino, S. A.; Somlai, C.; Cszimadia, I. G.; Penke, B.; Enriz, R. D. *Bioorg. Med. Chem.* **2006**, *14*, 7604.
- Masman, M. F.; Somlai, C.; Garibotto, F. M.; Rodríguez, A. M.; de la Iglesia, A.; Zacchino, S. A.; Penke, B.; Enriz, R. D. *Bioorg. Med. Chem.* **2008**, *16*, 4347.
- Zaslöf, M. *Curr. Opin. Immunol.* **1992**, *4*, 3.
- Ganz, T.; Lehrer, R. I. *Pharmacol. Ther.* **1995**, *66*, 191.
- Hoffman, J. A.; Kafatos, F. C.; Janeway, C. A., Jr.; Ezekowitz, R. A. B. *Science* **1999**, *284*, 1313.
- Hancock, R. E. W.; Patrzykat, A. *Curr. Drug Targets Infect. Disord.* **2002**, *2*, 79.
- Masman, M. F.; Rodríguez, A. M.; Raimondi, M.; Zacchino, S. A.; Luiten, P. M. G.; Somlai, C.; Kortvelyesi, T.; Penke, B.; Enriz, R. D. *Eur. J. Med. Chem.* **2009**, *44*, 212.
- Schiffer, M.; Chang, C.-H.; Stevens, F. J. *Protein Eng.* **1992**, *5*, 213.
- Derossi, D.; Joliot, A. H.; Chassaing, G.; Prochiantz, A. *J. Biol. Chem.* **1994**, *269*, 10444.
- Ripoll, D. R.; Scheraga, H. A. *Biopolymers* **1988**, *27*, 1283.
- Némethy, G.; Gibson, K. D.; Palmer, K. A.; Yoon, C. N.; Paterlini, G.; Zagari, A.; Rumsey, S.; Scheraga, H. A. *J. Phys. Chem.* **1992**, *96*, 6472.
- Chemical Applications of Atomic and Molecular Electrostatic Potentials*; Politzer, P., Truhlar, D. G., Eds.; Plenum Press: New York, 1991.
- Náray-Szabó, G.; Ferenczy, G. G. *Chem. Rev.* **1995**, *95*, 829.
- Christiaens, B.; Grooten, J.; Reusens, M.; Joliot, A.; Goethals, M.; Vandekerckhove, J.; Prochiantz, A.; Rosseneu, M. *Eur. J. Biochem.* **2004**, *271*, 1187.
- Clinical and Laboratory Standards Institute (CLSI, formerly National Committee for Clinical and Laboratory Standards NCCLS). Method M27-A2, 2nd ed.; Wayne, Ed., 2002; Vol. 22, pp 1–29.
- Pfaller, M. A.; Diekema, D. J. *Clin. Microbiol. Rev.* **2007**, *20*, 133.
- Drin, G.; Mazel, M.; Clair, P.; Mathieu, D.; Kaczorek, M.; Tamsamani, J. *Eur. J. Biochem.* **2001**, *268*, 1304.
- Brattwall, C. E. B.; Lincoln, P.; Nordén, B. *J. Am. Chem. Soc.* **2003**, *125*, 14214.
- Lensink, M. F.; Christiaens, B.; Vandekerckhove, J.; Prochiantz, A.; Rosseneu, M. *Biophys. J.* **2005**, *88*, 939.
- Bisogno, F.; Mascotti, M. L.; Sanchez, C.; Garibotto, F.; Giannini, F.; Kurina Sanz, M.; Enriz, R. D. *J. Agric. Food Chem.* **2007**, *55*, 10635.
- Freile, M.; Giannini, F.; Sortino, M.; Zamora, M.; Juárez, A.; Zacchino, S.; Enriz, R. D. *Acta Farm. Bonaerense* **2006**, *25*, 83.
- Mascotti, M. L.; Enriz, R. D.; Giannini, F. A. *Lat. Am. J. Pharm.* **2008**, *27*, 904.
- Shai, Y. *Biopolymers* **2002**, *66*, 236.
- Huang, H. W. *Biochemistry* **2000**, *39*, 8347.

41. Kaiser, E.; Colescott, R. L.; Bossiuger, C. D.; Cook, P. I. *Anal. Biochem.* **1970**, *34*, 595.
42. Johnson, W. W.; Finley, M. T. *Handbook of Acute Toxicity of Chemicals to Fish and Aquatic Invertebrates*. United States Department of the Interior Fish and Wildlife Service; 1980, Resource Publication 137. Washington, DC, pp 1–8.
43. Slooff, W.; De Zwart, D.; Van de Kerkhoff, J. *Aquat. Toxicol.* **1983**, *4*, 189.
44. Liwo, A.; Tempczyk, A.; Oldziej, S.; Shenderovich, M. D.; Hruby, V. J.; Talluri, S.; Ciarkowski, J.; Kasprzykowski, S.; Lankiewicz, L.; Grzonka, Z. *Biopolymers* **1996**, *38*, 157.
45. Ripoll, D. R.; Scheraga, H. A. *Biopolymers* **1990**, *30*, 165.
46. Scheraga, H. A.; Ripoll, D. R.; Liwo, A.; Czaplewski, C. User Guide ECEPPAK and ANALYZE Programs.
47. Vila, J.; Williams, R. L.; Vásquez, M.; Scheraga, H. A. *Proteins Struct. Funct. Genet.* **1991**, *10*, 199.
48. Williams, R. L.; Vila, J.; Perrot, G.; Scheraga, H. A. *Proteins Struct. Funct. Genet.* **1992**, *14*, 110.
49. Frisch, M. J.; Trucks, G. W.; Schlegel, H. B.; Scuseria, G. E.; Robb, M. A.; Cheeseman, J. R.; Montgomery, J. A., Jr.; Vreven, T.; Kudin, K. N.; Burant, J. C.; Millam, J. M.; Iyengar, S. S.; Tomasi, J.; Barone, V.; Mennucci, B.; Cossi, M.; Scalmani, G.; Rega, N.; Petersson, G. A.; Nakatsuji, H.; Hada, M.; Ehara, M.; Toyota, K.; Fukuda, R.; Hasegawa, J.; Ishida, M.; Nakajima, T.; Honda, Y.; Kitao, O.; Nakai, H.; Klene, M.; Li, X.; Knox, J. E.; Hratchian, H. P.; Cross, J. B.; Bakken, V.; Adamo, C.; Jaramillo, J.; Gomperts, R.; Stratmann, R. E.; Yazyev, O.; Austin, A. J.; Cammi, R.; Pomelli, C.; Ochterski, J. W.; Ayala, P. Y.; Morokuma, K.; Voth, G. A.; Salvador, P.; Dannenberg, J. J.; Zakrzewski, V. G.; Dapprich, S.; Daniels, A. D.; Strain, M. C.; Farkas, O.; Malick, D. K.; Rabuck, A. D.; Raghavachari, K.; Foresman, J. B.; Ortiz, J. V.; Cui, Q.; Baboul, A. G.; Clifford, S.; Cioslowski, J.; Stefanov, B. B.; Liu, G.; Liashenko, A.; Piskorz, P.; Komaromi, I.; Martin, R. L.; Fox, D. J.; Keith, T.; Al-Laham, M. A.; Peng, C. Y.; Nanayakkara, A.; Challacombe, M.; Gill, P. M. W.; Johnson, B.; Chen, W.; Wong, M. W.; Gonzalez, C.; Pople, J. A. *GAUSSIAN 03*, Revision B.01; Gaussian, Inc.: Wallingford, CT, 2004.
50. Flükiger, P.; Lüthi, H. P.; Portmann, S.; Weber, J. *MOLEKEL 4.0*, Swiss Center for Scientific Computing, Manno, Switzerland, 2000.